A Novel Approach for Image Denoising Based on Artificial Neural Networks

Şeref SAĞIROĞLU*, Erkan BEŞDOK**

*Gazi University, Engineering Faculty, Computer Engineering Department, Maltepe, 06570, Ankara, Turkey
**Erciyes University, Engineering Faculty, Geodesy Photogrammetry
Engineering Department, Talas Yolu, 38050, Kayseri, Turkey

ABSTRACT

This study presents a novel approach based on artificial neural networks (ANNs) to remove noises from defected images. ANNs were trained with two different learning algorithms, Levenberg-Marquardt and Extended-Delta-Bar-Delta, for speeding up the training and feedforward calculation processes. The restored results were also compared to the classical techniques, FFT, Wiener+Median filtering and wavelet denoising. The results were shown that the proposed novel neural model provides simplicity and accuracy to remove noises from defected images without estimating any mathematical model than the others.

Key Words: Image Restoration, Wavelet, Wiener, Median, FFT, Artificial neural networks.

Görüntülerde Gürültü Gidermek için Yapay Sinir Ağı Tabanlı Yeni Bir Yaklaşım

ÖZET

Bu çalışma, bozulmuş görüntülerden gürültüleri temizlemek için yapay sinir ağları (YSA) tabanlı yeni bir yaklaşım sunar. YSA'ların öğrenme hızını ile ileri yönde hesaplama işlemlerini arttırmak için Levenberg-Marquardt ve genişletilmiş Delta-Bar-Delta algoritmaları ile eğitilmiştir. YSA modelleriyle onarılan görüntüler, literatürdeki klasik teknikler, FFT, Wiener+Median filtreleme and Wavelet gürültü giderici ile de karşılaştırılmıştır. Elde edilen sonuçlar göstermiştir ki çalışma kapsamında sunulan yeni yaklaşımın herhangi bir matematiksel model kullanılmaksızın bozulmuş görüntülerden basit ve başarılı bir şekilde gürültüleri temizlediği görülmüştür.

Anahtar Kelimeler: Görüntü Onarımı, Dalgacık Dönüşümü, Wiener, Median, FFT, Yapay Sinir Ağları.

I. INTRODUCTION (GİRİŞ)

In general, images are restored if they are distorted by a system or mechanism during measurements. Motion blur, noise, out-of-focus blur, distortion caused by low resolution are some of the degradation caused the systems or the mechanisms. The main idea of restoration is to reconstruct an image from its degraded one or to retrieve meaningful information from degraded images [Elad and Feuer 1997; Li 1998]. Blurring due to optical system aberrations, diffraction, motion, atmospheric turbulence in remote sensing, astronomy, scanning of photographs for critical tasks and film nonlinearities in digital photogrammetry, and also noises due to electronic imaging sensors, film granularity and atmospheric light fluctuations have been some of the problems encountered in image restorations [Chellappa and Kashyap 1982; Lee et al. 1990; Baltsavias 1994; Baltsavias and Bill 1994; Baltsavias and Kaeser 1994; Murtagh et al. 1995; Banham and Katsaggelos 1996].

In general, distortions in images can be classified into two categories [Andrews and Hunt 1977; Gonzales and Woods 1992]. Some distortions may be described as spatially invariant or space invariant. All pixels have suffered the same form of distortion in a space invariant distortion. General distortions are named as spatially variant or space variant. In a space variant distortion, the degradation suffered by a pixel in the image depends upon its location in the image. In addition, image degradations can be described as linear or non-linear [Andrews and Hunt 1977]. In this work, distortions which may be described by a linear model are considered. For accurate image restoration, the degradation function must be known. Lack of sufficient information about degradation and difficulty in estimating degradation type and/or parameters are the problems or the difficulties encountered in practical applications [Chellappa and Kashyap 1982; Lagendijk et al.1988; Galatsanos and Chin 1991; Perez-Minana et al.1993; Banham and Katsaggelos 1996; Kundur and Hatzinakos 1996].

Most image restoration methods use convolution applied to the entire image and can be classified into two groups: deterministic and stochastic. Deterministic methods are applied to images with a known degradation function and specified level of noise [Chellappa and Kashyap 1982; Banham and Katsaggelos 1996; Kundur and Hatzinakos 1996]. The

Sorumlu Yazar (Corresponding Author)
e-posta: ss@gazi.edu.tr
Digital Object Identifier (DOI) : 10.2339/2012.15.2, 71-86

original image is obtained from the degraded one by a transformation inverse to the degradation in these methods. Stochastic methods provide best restoration with the help of a particular criterion [Perez-Minana et al. 1993; Woo et al. 1993].

There have been many image restoration techniques available in the literature [Tekalp and Pavlovic 1990; Woo et al. 1991; Perez-Minana et al. 1993; Schomberg and Timmer 1995; Kundur 1995; Wang et al. 1995; Kundur and Hatzinakos 1996; Flusser and Suk 1998; Huang and Woolsey 2000; Chang et al. 2000a; 2000b; Keller et al. 1993; Krell et al. 1996; Wong and Guan 1997; Barto et al. 1995; Celebi and Guzelis 1997; Zhao and Yu 1999; Steriti and Fiddy 1993; Egmont-Peterson et al. 2002; Zhou et al. 1988; Skrzypek and Karpluz 1992; Guan 1996; Ansari and Zhang 1993; Bedini and Tonazzini 1992; Chua and Wang 1988a; Chua and Wang 1988b; Ridder et al. 1999; Figueiredo and Leitao 1994; Greenhill and Davies 1994; Guan 1997; Hanek and Ansari 1996; Lee and Degyvez 1996; Nosak and Roska 1993; Paik and Katsaggelos 1992; Phoha and Oldham 1996; Qian et al. 1993; Sun and Yu 1995; Zamparelli 1997; Zhang and Ansari 1996]. Transform related restoration techniques (inverse filter, Wiener filter, parametric estimation filter, Kalman filter, homomorphic filter), algebraic restoration techniques (pseudo inverse spatial image restoration, singular value decomposition, Wiener estimation, constrained image restoration) and recently artificial intelligence techniques (neural networks, fuzzy logic and genetic algorithm) have been applied to image restoration. Some of these methods, Wiener filter (WF) [Wang et al. 1995; Huang and Woolsey 2000], Kalman Filter [Tekalp and Pavlovic 1990; Liguni et.al 1992; Azimisadjadi et al. 1999], Inverse filtering based on the properties of Fourier transform [Schomberg and Timmer 1995], Wavelet transform denoising [Banham and Katsaggelos 1996; Chang et al. 2000a; 2000b; Zhang and Nosratinia 2000] with the coefficient-wise or pixel-wise operations and many other model-based classical approaches [Strak 1987] have been applied to restore images. Most of these methods have been the modified or/and extended versions of those.

Fourier transforms (FTs) have been used extensively for image signal processing [Wilson et.al 1992; Weng 1993]. The Fourier transform is linear and associative under addition, but is not associative under multiplication. In this respect, FTs are suitable for removing noise from images only when the noise can be modelled as an additive term to the original image. If a defect such an uneven lighting has to be modelled as multiplicative rather than additive, direct application of Fourier methods is inappropriate.

Wiener+Median filters (WMFs) have been also applied extensively to image restoration and signal processing [Schomberg and Timmer 1995, Wang et al. 1995, Huang and Woolsey 2000]. WMFs are used to improve frequency domain deconvolution, to formulate the in-class image and the out-of-class noise image into a single step filter construction and to restore reference objects in a fractional correlation system [Wang et al. 1995; Huang and Woolsey 2000]. Wavelet thresholding (WT) has been the recent method used in image restoration [Chang et al. 2000a; 2000b; Zhang and Nosratinia 2000].

Artificial neural networks (ANNs) have been applied many areas successfully because of their ability to learn, ease of implementation and fast real-time operation [Simpson 1990, Haykin 1994, Neuralware 1996, Ripley 1996, Demuth and Beale 1998]. Different network topologies and learning algorithms have been investigated to restore images [Paik and Katsaggelos 1992; Keller et al. 1993; Steriti and Fiddy 1993; Barto et.al 1995; Celebi and Guzelis 1996; Krell et al. 1996; Wong and Guan 1997; Zhao and Yu 1999]. Multilayered perceptrons, learning vector quantisation network, cellular neural network, Hopfield network, wavelet-based neural network and model-based neural network have been mostly used neural network structures for image restorations. All of those works, cost functions have been minimized. In this work, instead of minimizing the cost function, a novel approach based on artificial neural network has been proposed to restore images with an estimated model.

In this paper, Section 2 presents a brief review on classical and ANN based image restoration techniques. Section 3 introduces artificial neural networks and their learning algorithms used in this work. Section 4 demonstrates the ANN approach presented in this study. The results obtained from this study are given in Section 5. The work is finally concluded in Section 6.

2. IMAGE RESTORATION TECHNIQUES
(RESİM İYİLEŞTİRME TEKNİKLERİ)

A general form of digital image restoration system is illustrated in Figure 1. As shown in Figure 1, an image is first acquired from the outside world. The acquired image is then restored from noisy or blurred image using a restoration technique. The image restoration techniques have been employed to remove deterministic or statistical degradations in the image restoration system [Strak 1987].

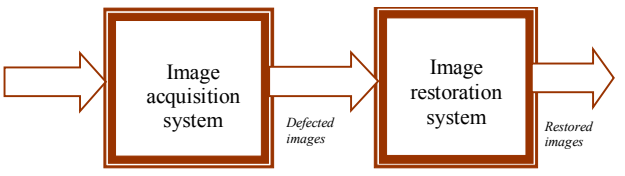

Figure 1. An image restoration system (Bir resim iyileştirme sistemi)

Linear image degradations can be described by their impulse responses. Consider a PSF of size P by P acting on an image of size N by M. In the case of a two-dimensional image, the PSF may be written as h(x,y). When noise is also present in the degraded image, the image degradation model in the discrete case becomes [Andrews and Hunt 1977]:

$$g(x,y)=\sum_{i}^{N}\sum_{j}^{M} f(i,j)\,h(x,y;i,j)+n(x,y) \qquad (1)$$

where *f(i,j)*and *g(x,y)* are the original and degraded images respectively, and *n(x,y)*is the additive noise component of the degraded image. If *h(x,y)*is a linear function then by lexicographically ordering *g(x,y)*, *f(i,j)* and *n(x,y)*into column vectors of size *NM*, Eqn (1) is then represented as a matrix operation [Andrews and Hunt 1977; Gonzales and Woods 1992]:

$$g = Hf + n \qquad (2)$$

where g and f are the lexicographically organised degraded and original image vectors, n is the additive noise component and H is a matrix operator whose elements are an arrangement of the elements of h(x,y) such that the matrix multiplication of f with H performs the same operation as convolving f(x,y) with h(x,y). The degradation measure starts with the constrained least square error measure [Gonzales and Woods, 1992]:

$$E=\frac{1}{2}\left\|g-H\hat{f}\right\|^2+\frac{1}{2}\beta\left\|D\hat{f}\right\|^2 \qquad (3)$$

where $\hat{f}$ is the restored image estimate, β is a constant, and D is a smoothness constraint operator. Since H is often a low pass distortion, D will be chosen to be a high pass filter. The second term in Eqn (3) is the regularisation term. Existing more noise in an image makes the second term in Eqn (3) larger, hence minimising the second term will involve reducing the noise in the image at the expense of restoration sharpness. Choosing β becomes an important consideration when restoring an image. Any large value of β will oversmooth the restored image, whereas very small a value of β will not properly suppress noise.

As briefly mentioned earlier sited in this article, there have been many image restoration techniques available in the literature. Frequency domain filtering (FDF), Wiener+Median filter (WM), and wavelet denoising (WD) techniques have been mostly preferred classical techniques in applications [Wang et al. 1995; Huang and Woolsey 2000; Chang et al. 2000a; 2000b; Zhang and Nosratinia 2000; Wilson et al. 1992]. Artificial neural networks have been also recently employed to intelligent image restoration [Liguni et.al 1992; Azimisadjadi et al. 1999; Egmont-Peterson et al. 2002; Tekalp and Pavlovic 1990; Woo et al. 1991; Demuth and Beale 1998; Perez-Minana et al. 1993; Schomberg and Timmer 1995; Kundur 1995; Wang et al. 1995; Kundur and Hatzinakos 1996; Flusser and Suk 1998; Huang and Woolsey 2000; Chang et al. 2000a; 2000b; Keller et al. 1993; Krell et al. 1996; Wong and Guan 1997; Barto et al. 1995; Celebi and Guzelis 1997; Zhao and Yu 1999; Steriti and Fiddy 1993; Egmont-Peterson et al. 2002; Zhou et al. 1988; Skrzypek and Karpluz 1992; Guan 1996; Ansari and Zhang 1993; Bedini and Tonazzini 1992; Chua and Wang 1988a; Chua and Wang 1988b; Ridder et al. 1999; Figueiredo and Leitao 1994; Greenhill and Davies 1994; Guan 1997; Hanek and Ansari 1996; Lee and Degyvez 1996; Nosak and Roska 1993; Paik and Katsaggelos 1992; Phoha and Oldham 1996; Qian et al. 1993; Sun and Yu 1995; Zamparelli 1997; Zhang and Ansari 1996].

The techniques taken into account in this work, FDF, WMF, WD and neural approaches used in this work, have been briefly introduced in the following subsections.

2.1. Frequency Domain Filtering (FDF)
(Frekans Alanı Filtrelemesi)

This is achieved with the Fourier transform (FT) representation of images [Schomberg and Timmer 1995; Sonka et al. 1999]. This transform is performed on three spatial domain functions: the degraded image, degradation function and the noise model. FDF is then applied to FT as

$$F(u,v)=\frac{1}{MN}\sum_{a=0}^{M-1}\sum_{b=0}^{N-1}\hat{f}(a,b)\,e^{-j2\pi(ua/M+vb/N)} \qquad (4)$$

The restored image is finally obtained from an inverse FT after some of the FT coefficients, considered as noise, are neglected as

$$f(a,b)=\frac{1}{MN}\sum_{a=0}^{M-1}\sum_{b=0}^{N-1}\hat{F}(u,v)\,e^{-j2\pi(ua/M+vb/N)} \qquad (5)$$

where F(u,v) represents f(a,b) in frequency domain.

2.2 Wiener+Median Filter (WMF)
(Wiener+Median Filtresi)

This filtering is also known as 'minimum mean-squared estimator' and alleviates some of the difficulties inherent in inverse filtering by attempting to model the error in the restorated image through with the use of statistical methods [Vrhel and Unser 1999]. This estimation model is

$$d(i,j)=\mu+\frac{\upsilon^2-\nu^2}{\upsilon^2}(\hat{f}(a,b)-\mu) \qquad (6)$$

where

$$\mu=\frac{1}{NM}\sum_{a,b\in\eta}\hat{f}(a,b) \qquad (7)$$

$$\upsilon^2=\frac{1}{NM}\sum_{a,b\in\eta}\hat{f}^2(a,b)-\mu^2 \qquad (8)$$

In Eqns (7) and (8), η is N-by-M local neighborhood of each pixel in the image f(a,b). ν^2 is the noise variance, and μ is the mean of noise. If the noise variance is not given WF uses the average of all the local estimated variances. The smoothing step is then applied for removing the rested defects [Huang and Woolsey 2000; Zhang and Nosratinia 2000].

The median filter is a nonlinear filter and operates on a local neighbourhood. After the size of the local neighbourhood is defined, the centre pixel is

replaced with the median or centre value present among its neighbours, rather than by their average. 3x3 size of neighbourhood has been selected in this work. Wiener+Median (WM) process is achieved by applying the Median filter operator onto the response of Wiener filter.

2.3. Wavelet Denoising (WD) (Dalgacık Gürültü Temizleme)

Wavelets are other approaches to represent decomposing complex signals into sums of basis functions, in this respect, they are similar to Fourier decomposition approaches, but they have an important difference [Huang and Woolsey 2000; Chang et al. 2000a; 2000b; Zhang and Nosratinia 2000]. Wavelets are derived from a basis function f(t) and a signal can be expressed as

$$f(t) = \sum_k \sum_i c_{i,k}(t)\psi_{i,k}(t) \tag{9}$$

where $\psi_{i,k}(t)$ is the orthonormal bases and $c_{i,k}(t)$ is the wavelet coefficients.

The wavelet thresholding can be applied and the image is then recovered from Eqn (10) given below in a simplified form as;

$$\hat{f} = f + \sigma v \tag{10}$$

where f is the original image signal, σ is the noise level of Gaussian white noise, υ is the noise level.

The mean square error of the estimation is minimised with a certain threshold. This offers better mathematical properties because it avoids discontinuities which otherwise is produced by the thresholding. Inverse wavelets are finally computed for accessing the restored images.

2.4. Neural Network Approaches (Yapay Sinir Ağı Yaklaşımları)

A recent survey covering more than 250 papers reports on applications of ANNs to image processing that image restoration was classified under the preprocessing as optimisation of an objective function defined by a classical preprocessing problem, approximation of a mathematical transformation used for image processing and mapping certain tasks [Egmont-Peterson et al. 2002]. In that report, the papers were evaluated under the processes; prepocessing, filtering, data reduction, feature extraction, segmentation, object detection and recognition, image understanding and optimization. Most of the majority of applications of ANNs in preprocessing can be found in image restoration [Egmont-Peterson et al. 2002].

ANNs have been applied to denoise or to restore defected or degradated images for many applications in the references [Egmont-Peterson et al. 2002; Tekalp and Pavlovic 1990; Woo et al. 1991; Demuth and Beale 1998; Perez-Minana et al. 1993; Schomberg and Timmer 1995; Kundur 1995; Wang et al. 1995; Kundur and Hatzinakos 1996; Flusser and Suk 1998; Huang and Woolsey 2000; Chang et al. 2000a; 2000b; Keller et al. 1993; Krell et al. 1996; Wong and Guan 1997; Barto et al. 1995; Celebi and Guzelis 1997; Zhao and Yu 1999; Steriti and Fiddy 1993; Egmont-Peterson et al. 2002; Zhou et al. 1988; Skrzypek and Karpluz 1992; Guan 1996; Ansari and Zhang 1993; Bedini and Tonazzini 1992; Chua and Wang 1988a; Chua and Wang 1988b; Ridder et al. 1999; Figueiredo and Leitao 1994; Greenhill and Davies 1994; Guan 1997; Hanek and Ansari 1996; Lee and Degyvez 1996; Nosak and Roska 1993; Paik and Katsaggelos 1992; Phoha and Oldham 1996; Qian et al. 1993; Sun and Yu 1995; Zamparelli 1997; Zhang and Ansari 1996]. In these references, various designs ranging from relatively simple to highly complex and modular approaches. In the basic image restoration approach, noise is removed from an image by simple filtering. In most applications, images are restored by the minimization of a cost function. It is achieved by using an ANN approach to optimize the cost function. This is very suitable for the iterative solution of the minimization approach to image restoration and the learning concept associated with ANN so this brings truly adaptive processing to restoration.

As mentioned earlier, image restoration using artificial neural network approaches is achieved to minimize a cost function associated with a neural network given by:

$$E = \frac{1}{2}\hat{f}^T W \hat{f} - b^T \hat{f} + c \tag{11}$$

Comparing this with Eqn (3), W, b, and c are functions of H, D, β and n and other problem related contraints. In terms of a neural network cost function, the (i,j)th element of W corresponds to the weights between neurons (pixels) i and j in the network. Similarly, vector b corresponds to the bias input to each neuron.

Equating the formula for the cost of a neural network with Eqn (3), the bias inputs and weights can be found such that as the neural network minimises its cost function, the image will be restored. If L=MN, weights and biases were then given as in [Zhou et al. 1998]:

$$w_{ij} = -\sum_{q=1}^{L} h_{qi}h_{qj} - \beta\sum_{q=1}^{L} d_{qi}d_{qj} \tag{12}$$

$$b_i = \sum_{q=1}^{L} g_q h_{qj} \tag{13}$$

where wij is the weights between pixels i and j, and bi is the bias input to neuron (pixel) i. In addition, hij is the (i,j)th element of matrix H from Eqn (2) and dij is the (i,j)th element of matrix D from Eqn (3).

There have been many available ANN training algorithms and structures used in image restoration. As mentioned earlier, backpropagation multilayered perceptron, modular neural network, cellular neural network and Hopfield network are the ANN structures used for restorations [Egmont-Peterson et al. 2002; Tekalp and Pavlovic 1990; Woo et al. 1991; Demuth and Beale 1998; Perez-Minana et al. 1993; Schomberg and Timmer 1995; Kundur 1995; Wang et al. 1995; Kundur and Hatzinakos 1996; Flusser and Suk 1998; Huang and Woolsey 2000; Chang et al. 2000a; 2000b; Keller et al. 1993; Krell et al. 1996; Wong and Guan 1997; Barto et al. 1995; Celebi and Guzelis 1997; Zhao and Yu 1999; Steriti and Fiddy 1993; Egmont-Peterson et al. 2002; Zhou et al. 1988; Skrzypek and Karpluz 1992; Guan 1996; Ansari and Zhang 1993; Bedini and Tonazzini 1992; Chua and Wang 1988a; Chua and Wang 1988b; Ridder et al. 1999; Figueiredo and Leitao 1994; Greenhill and Davies 1994; Guan 1997; Hanek and Ansari 1996; Lee and Degyvez 1996; Nosak and Roska 1993; Paik and Katsaggelos 1992; Phoha and Oldham 1996; Qian et al. 1993; Sun and Yu 1995; Zamparelli 1997; Zhang and Ansari 1996].

In the applications; Zhou et al.(1988) proposed a Hopfield neural network approach to a constrained mean square error estimation. The network was further optimized by Paik and Katsaggelos (1992) to remove the step where the energy reduction is checked the calculation of the change in the neuron state. Hopfield networks were also used to solve classical methods for more complex restoration problems [Bedini and Tonazzini 1992; Figueiredo and Leitao 1994; Paik and Katsagelos 1992]. Often, mapping the problem turned out to be difficult, so in some cases the network architecture had to be modified as well. Qian et al. (1993) developed a hybrid system consisting of order statistic filters for noise removal and a Hopfield network for deblurring by optimising a criterion function. The modulation transfer function had to be measured in advance. Steriti and Fiddy (1993) compared Hopfield network energy minimization approach to the singular value decomposition method of finding a matrix inverse and found that Hopfield network achieved the task in high accuracy.

Liguni et al. (1992) developed several new learning algorithms for a multilayered neural network based on the extended Kalman filter. Greenhil and Davies (1994) used a regression multilayered neural network in a convolution-like way to suppress noise. They achieved this with a 5×5 pixel window as input and one output node. A modular multilayered network was used to mimic the behaviour of the Kuwahara filter used for an edge-preserving smoothing filter [Ridder et al. 1999]. It was reported that the mean squared error achieved in training may not be representative of the problem at hand. Furthermore, unconstrained multilayered networks often ended up in a linear approximation to the Kuwahara filter.

Chua and Yang (1988a; 1988b;) used cellular neural networks for image processing. A cellular network is a system in which nodes are locally connected [Nossek and Roska 1993]. Each node contains a feedback template and a control template determining the functionality of the network. The templates implement an averaging function for noise suppression and a Laplacian operator for edge detection. The system operates locally, but multiple iterations allow it to distribute global information throughout the nodes. Zamparelli (1997) has proposed methods for training cellular neural networks using gradient descent or genetic algorithms. These networks were also applied for restoration of colour images by Lee and Degyvez (1996).

Another interesting ANN architecture is the generalized adaptive neural filter [Hanek and Ansari 1996; Zhang and Ansari 1996] which has been used for noise suppression. This neural filter consists of a set of neural operators, based on stack filters that uses binary decompositions of gray-level data [Ansari and Zhang 1993].

Guan et al. (1997) developed a so-called network-of-networks for image restoration. Their system consists of loosely coupled modules, where each module is a separate ANN. Phoha and Oldham (1996) proposed a layered competitive network to reconstruct a distorted image.

As can be seen from the references sited and explained earlier, there have been many available ANN training algorithms and structures used in image restoration. As aforementioned, multilayered perceptron, modular neural network, cellular neural Networks, Hopfield network and their hybrid and modular combinations are the neural structures used for image restoration. Multilayered perceptron neural networks have been mostly preferred ANN architecture used in the literature. This ANN structure is also used in this study to denoise destored images. The details of ANNs used in this work has been introduced in Section 3.

3. ARTIFICIAL NEURAL NETWORKS (YAPAY SİNİR AĞLARI)

Artificial neural networks (ANNs) represent promising modelling technique, especially for data sets having nonlinear relationships which are frequently encountered in the field of engineering. The various fields of engineering applications of ANNs can be summarised into classification, pattern recognition, prediction and modelling, identification, speech, vision and control systems [Simpson 1990; Haykin 1994; Demuth and Beale 1998].

Multilayered perceptron (MLP) is one of most and widely used ANN structure. As shown in Figure 2, an MLP consists of three layers: an input layer, an output layer and one or more hidden layers. Neurons in the input layer act only as buffers for distributing the input signal xi to neurons in the hidden layer. Each

neuron j in the hidden layer sums its input signals xi after multiplying them by the strengths of the respective connection weights wji and computes its output yj as a function of the sum. The function is usually a sigmoidal or hyperbolic tangent function. The outputs of neurons in the output layer are computed similarly.

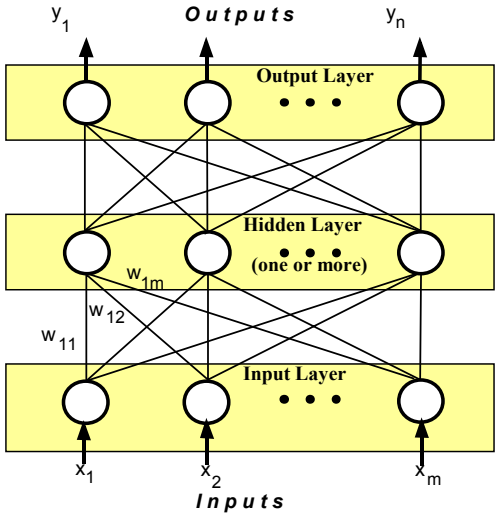

Fig.2 General form of MLPs (MLP'nin genel gösterimi)

Training a network consists of adjusting its weights using a training algorithm. The training algorithms adopted in this study optimise the weights by attempting to minimise an objective error function.

Each weight wji is adjusted by adding an increment Δwji to it. Δwji is selected to reduce E as rapidly as possible. The adjustment is carried out over several training iterations until a satisfactorily small value of E is obtained or a given number of iteration is reached. How Δwji is computed depends on the training algorithm adopted. Levenberg-Marquardt and Extended Delta-Bar-Delta (EDBD) are the learning algorithms for faster training or converge. These algorithms have been used in this work and briefly explained in the following subsections.

3.1. Levenberg-Marquardt Method (LMM)
(Levenberg-Marquardt Metodu)

Essentially, this is a least-squares estimation method based on the maximum neighbourhood idea [Marquardt 1963; Fletcher 1980; Gill et al. 1981]. The LMM combines the best features of the Gauss-Newton technique and the steepest-descent method, but avoids many of their limitations. In particular, it generally does not suffer from the problem of slow convergence.

Let E(w) be an objective error function made up of m individual error terms $e_i^2(w)$ as follows:-

$$E(w) = \sum_{i=1}^{m} e_i^2(w) = \left\| f(w) \right\|^2 \tag{14}$$

It is assumed that function f(.) and its Jacobian J are known at a point w. The aim of the LMM is to compute the parameter vector w such that E(w) is minimum. Using the LMM, a new vector wk+1 can be obtained from an estimated vector wk as follows:

$$wk+1 = w+\delta wk \tag{15}$$

where δwk is given by :

$$(J_k{}^T J_k + \lambda I) w \delta_k = J_k{}^T f(w_k) \tag{16}$$

In Eqn (16), J_k is the Jacobian of f evaluated at wk, λ is the Marquardt parameter and I is the identity matrix. Further information about the LMM and their applications can be found in the references [Marquardt 1963; Fletcher 1980; Gill et al. 1981; Bulsari and Saxen 1991; Pham and Sagiroglu 1996].

3.2. Extended Delta-Bar-Delta (EDBD) Algorithm (Genişletilmiş Delta-Bar-Delta Algoritması)

As its name implies, this algorithm [Neuralware 1996] is an extension of Delta-Bar-Delta [Haykın 1994]. Aimed at speeding up the training of MLPs, the EDBD is based on the hypothesis that learning and momentum coefficients suitable for one weight may not be appropriate for all weights. By assigning a learning coefficient and a momentum coefficient to each weight and permitting it to change over time, more freedom is introduced to facilitate convergence towards a minimum value of E(w_{ji}). The changes in weights are calculated as:

$$\Delta w_{ji}(k) = -\alpha_{ji}(k) \frac{\partial E(k)}{\partial w_{ji}(k)} + \mu_{ji}(k) \Delta w_{ji}(k-1) \tag{17}$$

where $\alpha_{ji}(k)$ and $\mu_{ji}(k)$ are learning and momentum coefficients, respectively.

The use of momentum in the EDBD is one of the differences between it and DBD. The learning coefficient change is given as:

$$\Delta\alpha_{ji}(k) = \begin{cases} A_\alpha \exp\left(-\gamma_\alpha \left| D_{ji}(k) \right|\right) & D_{ji}(k-1) \dfrac{\partial E}{\partial w_{ji}(k)} > 0 \\ -\varphi_\alpha \alpha_{ji}(k) & D_{ji}(k-1) \dfrac{\partial E}{\partial w_{ji}(k)} < 0 \\ 0 & \text{otherwise} \end{cases} \tag{18}$$

where A_α, γ_α and φ_α are the positive constants. $D_{ji}(k-1)$ represents a weighted average of $\partial E/\partial w_{ji}(k-1)$ and $\partial E/\partial w_{ji}(k-2)$ given by

$$D_{ji}(k-1) = (1-\theta) \frac{\partial E}{\partial w_{ji}(k-1)} + \theta \frac{\partial E}{\partial w_{ji}(k-2)} \tag{19}$$

The momentum coefficient change is obtained as:

$$\Delta\mu_{ji}(k) = \begin{cases} A_\mu \exp\left(-\gamma_\mu \left| D_{ji}(k) \right|\right) & D_{ji}(k-1) \dfrac{\partial E}{\partial w_{ji}(k)} > 0 \\ -\varphi_\mu \mu_{ji}(k) & D_{ji}(k-1) \dfrac{\partial E}{\partial w_{ji}(k)} < 0 \\ 0 & otherwise \end{cases} \tag{20}$$

where A_μ, γ_μ and φ_μ are the positive constants. Note that increments in the learning coefficient are not constant, but vary as an exponentially decreasing function of the magnitude of the weighted average gradient component $D_{ji}(k)$. To prevent oscillations in the values of the weights, $\alpha_{ji}(k)$ and $\mu_{ji}(k)$ are kept below preset upper bounds αmax and μmax.

4. IMAGE RESTORATION BASED ON ARTIFICIAL NEURAL NETWORKS (YAPAY SİNİR AĞI TEMELLİ RESİM İYİLEŞTİRME)

ANNs are known to overcome many problems in modelling, identification, control, filtering, recognition and classification. When ANN based image restorations have been reviewed, it has been generally found that the established models have been based on estimating the parameters of the present models. In this article, ANN based approach has been also applied to image restoration. In stead of establising a mathematical model, parameters or a rough model based on ANN has been introduced to restore images with the help of ANN features such as learning nonlinearity, generalising and fast computation and filtering. The proposed approach, training and test data sets, structures and parameters of ANN models, measuring restoration performance were introduced in the following subsections.

4.1. Proposed Novel Approach (Önerilen Yeni Yaklaşım)

As mentioned earlier, there have been a number of different ways available in the literature to restore noisy images. In contrast to the earlier method illustrated in Section 2.4, the noise in images are restored using a proposed neural model which learns how to remove the noise from corrupted images.

How an noisy, corrupted or blurred image can be restored using ANN approach presented in this work step by step. Using the steps (1)-(7) given below, the restoration is achieved smoothly.

(1) A neural network model is set up according to the parameters (ANN architecture, learning algorithm, no of inputs, no of outputs, no of processing elements, etc.)

(2) Preparing training and test sets (Please see Section 4.2 for more details).

i. An expert roughly estimates the noise level of a defected image with naked eyes.

ii. A texture pair is selected.

iii. According to the estimation, some noise was inserted into one of the image texture pair.

iv. A texture pair (image and noise inserted image) is prepared for ANN training.

v. According to (ii)-(iii), new texture pairs having different textures and noise levels are produced as much as needed.

(3) The both of the noise inserted image and the image were used to train an ANN model to remove the noise from the noisy image. In this step, the image texture having noise was apllied to an ANN model and the image texture having no noise was used as an output in the training processes.

(4) According to the inputs applied to the ANN model, ANN produces an output. The error is calculated between the desired output and actual output with the help of Eqn (14) or Eqn (21).

(5) The calculated errors were then used for training process of ANN with the help of a learning algorithm to learn the relationship among the noisy image and the image without noise.

(6) The learning process continues until a satisfactory result is achieved.

(7) A well-trained ANN model was then used to test the texture images having different level of noises and defects. It should be reminded that the test images were unknown or unseen by a well-trained ANN.

The block diagram used for noise removal with the help of ANN is given in Figure 3. ANN models in this work are supposed to learn the relations between the noisy input vectors and the output vectors having no noise. An ANN model simply learns how to remove or filter the noise from the texture pairs established using a learning algorithm based on a cost function. During the test phase, the noise or undesired effect can be then removed or filtered by ANN models from any defected image.

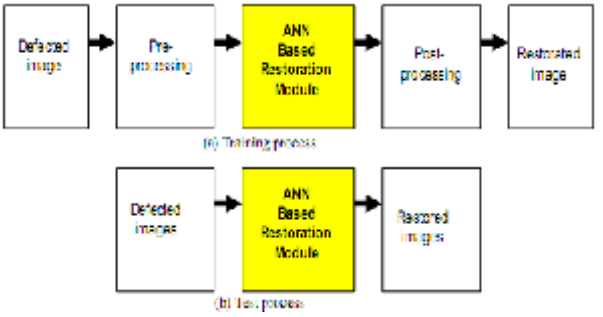

Figure 3. An image restoration system with ANN. (YSA ile görüntü iyileştirme sistemi)

The parameters of ANN modela are adjusted according to the error measure as:

$$E = \left\| g - (H\hat{f} + n) \right\| = d_k(n) - y_k(n) \qquad (21)$$

where $d_k(n)$ is the desired output node k at iteration n and $y_k(n)$ is the output of the output node k at iteration n. The relations among ANN parameters and other methods can be followed from Eqns (3), (11) and (14). In this study, ANN parameters were adjusted to minimize the errors using Eqns (16) and (17).

To train and test the ANN models, the texture pairs prepared earlier were used in these processes as shown in Figures 4-9.

In order to implement and test the approach, six different texture image pairs were prepared. The texture pairs used in this work are given in Figures 4-9. Different levels of noises like the salt-and-pepper were

then inserted into these textures. These pairs were then used to train the neural models for better restoration. It is seen that establishing an appropriate training texture and designing a suitable ANN structure are important and crucial for a proper restoration. The proposed ANN filter is a three-layered ANN with inputs derived from an NxN neighborhood of the transformed image and appropriately selected neuron activation functions.

(a) input vectors (b) output vectors

Figure 4. Texture pairs used in training (set#1) (Eğitimde kullanılan görüntü çiftleri)

(a) input vectors (b) output vectors

Figure 5. Texture pairs used in training (set#2) (Eğitimde kullanılan görüntü çiftleri)

(a) input vectors (b) output vectors

Figure 6. Texture pairs used in training (set#3) (Eğitimde kullanılan görüntü çiftleri)

(a) input vectors (b) output vectors

Figure 7. Texture pairs used in training (set#4) (Eğitimde kullanılan görüntü çiftleri)

(a) input vectors (b) output vectors

Figure 8. Texture pairs used in training (set#5) (Eğitimde kullanılan görüntü çiftleri)

(a) input vectors (b) output vectors

Figure 9. Texture pairs used in training (set#6) (Eğitimde kullanılan görüntü çiftleri)

4.2. Establishing Training and Test Data Sets
(Eğitim ve Test Veri Kümelerinin Oluşturulması)

In order to improve and test the ANN performances for the restoration, six random design textures were established to train ANNs with different level of noises inserted into images as shown in Figures 4-9. The similarity measures of training sets were computed and given in Table 1. These sets from 1 to 6 were represented as Set#1, Set#2, Set#3, Set#4, Set#5 and Set#6. Each set was used to train only one ANN model. Noise inserted textures in Figures 4-9 were used as inputs to the ANN models. Textures without noise or noiseless textures in Figures 3-8 were also applied to the ANN models as the desired outputs.

Table 1. Similarity measures for training sets. (Eğitim kümesi için benzerlik ölçüm sonuçları).

Training sets	**Similarity Measure C**
Set#1	0.93836
Set#2	0.93906
Set#3	0.83466
Set#4	0.85587
Set#5	0.76849
Set#6	0.85408

Two preprocessing procedures, the window-to-window (WTW) and the window-to-pixel (WTP), were applied to the six texture pairs to obtain better performance from neural models. The WTW method is based on the unoverlapping window of the images used for establishing the data sets. One input window matches to the one output window in the same spatial position. The WTP is also based on the overlapping window of input textures and matching these inputs with the pixels at the central position of the window on the output textures.

The images in Figure 10 were used to test the performances of the classical techniques and ANN models trained with the LMM and the EDBD algorithms. The similarity measure was 0.91066. When the test image elaborated in Figure 10(b) obeys a Gaussian curve with the standard deviation ν=0.3044 and the mean μ=0.5024. It is clear from Figure 11 that the noise occurs independently, the spatial positions illustrated with black in the figure suffer from unexpected noises with the level 0.93%. It can be finally said that the noise is spatially independent and fully random.

Rectangular windows have been mostly preferred in image processing for tasks such as smoothing. While rectangular windows are efficient, they yielded poor results near object boundaries as stated by Boykov et al. (1998). In this work, 3x3 and 5x5 sized image windowing were used to compare the

effects of the window sizes on ANN training performance for the image restoration.

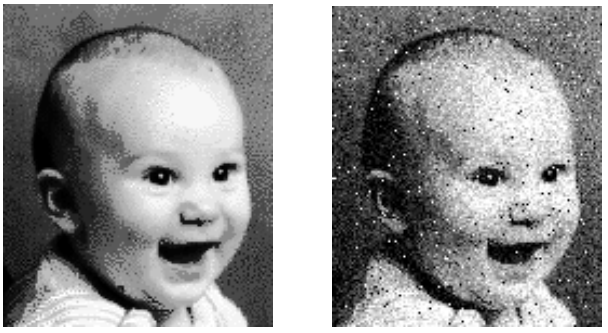

(a) original (b) defected

Figure 10. Test images. (Test resimleri)

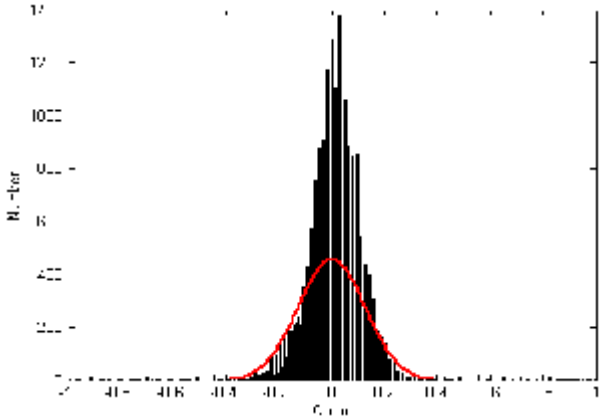

(a) standard deviation

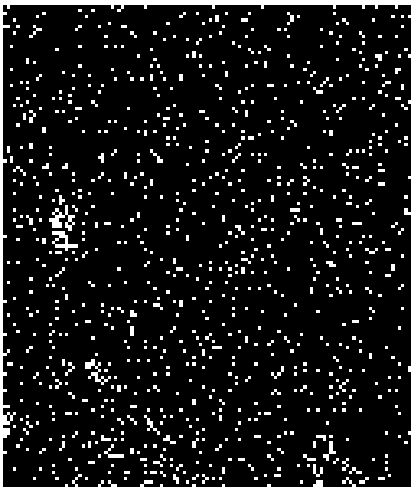

(b) Spatial position of defected pixels with black

Figure 11. Random noise characteristics of the defected image in Fig. 10(b) (Şekil 10(b)'de verilen bozulmuş resimlerin rasgele gürültü karakteristikleri)

4.3. ANN Structure and Parameters (YSA Yapısı ve Parametreleri)

In order to show the success of the proposed approach involves training twenty-eight ANN models including two training algorithms and preprocessing procedures to restore the texture pairs given in Figures 4-10. As explained before two learning algorithms, the EDBD and the LMM, were used to train ANNs. The ANNs trained with the LMM had the linear transfer function in the input layer and the tangent hyperbolic function in the hidden and output layers. The other twelve ANNs trained with EDBD algorithm had the linear transfer function in the input layer, the sigmoid functions in the hidden and the output layers. The rest four neural models were used to test the window sizes. Training the ANN models by two learning algorithms to restore the six texture pairs involves presenting them sequentially with the different set of vectors (inputs) and the corresponding vectors (outputs) as given in Figures 4-9.

The differences between the desired output vectors and the actual outputs of the ANNs are used to adjust the weights of ANN models through a learning algorithm. The adjustment is carried out after presenting each set until the restoration accuracy of the network is deemed satisfactory according to the error of the cost function given in Eqn (14) for all the training sets that fall below 0.001 or the maximum allowable number of epochs is reached to 100 for the LMM. The epoch is the number of training cycle. The training is stopped if the error is stable or did not change any more in the EDBD training.

A set of random values distributed uniformly between -0.1 and +0.1 were used to initialize the weights of the twenty-four ANN models. However, for the ANN trained with LMM, the input and the output data vectors were scaled between 0 and 1.0. For the ANN trained with EDBD, the input data vectors were scaled between 0 and 1.0 and output data vectors were also scaled between 0.2 and 0.8. After several trials, it was found that ANN having one hidden layer achieved the task within high accuracy. The suitable network configurations for having the LMM and EDBD training algorithms found were 9x10x1 (input x hidden x output) neurons for the WTP method. For 3x3 image sized unoverlapping with the WTW method, the ANN structures having EDBD and LMM algorithms were 9x10x9 (input x hidden x output) neurons and 9x5x9 (input x hidden x output) neurons, respectively.

The parameters of the networks are: for the LMM, λ=0.01; for the EDBD, A_α=0.095, A_μ=0.01, γ_μ=0.0, γ_α=0.0, φ_μ=0.01, φ_α=0.1, θ=0.7, λ=0.2 and $\alpha_{max}=\mu_{max}$ 2.0.

4.4. Measuring Restoration Performances (İyileştirme Performansının Ölçülmesi)

Many classical image restoration cost functions are based on the mean square error (MSE). This error measure helps to compare images on a pixel-to-pixel basis and, in fact, makes a statement about the power of the noise signal created by subtraction of the two images to be compared. The aim of this comparison is to produce a measure with which human beings will evaluate the quality of the image processed. Signal-to-Noise Ratio (SNR), Mean-Squared-Error (MSE) and Correlation (C) are the measures mostly used in

literature to compare the performance level of the restoration [Edelstein 1986]. To provide reliable and compact evaluations to the researchers working on the restoration applications, these three image quality measures were employed in this work. Each of these measures signs for the success of restoration performance. The first similarity measure is the correlation (C) and is found from d and y spaces as:

$$C_{d,f} = \frac{\sum_{i=1}^{M}\sum_{j=1}^{N}\left(d_j^{(i)} - \hat{d}_j\right)\left(f_j^{(i)} - \hat{f}_j\right)}{\sqrt{\left(\sum_{i=1}^{M}\sum_{j=1}^{N}\left(d_j^{(i)} - \hat{d}_j\right)^2\right)\left(\sum_{i=1}^{M}\sum_{j=1}^{N}\left(f_j^{(i)} - \hat{f}_j\right)^2\right)}} \quad (22)$$

where f and d are the original and the restored image, respectively.

The second one is the SNR measure. This measure is the ratio of the noise removal [Moulin 1995; Sun et al. 2001] and is defined in decibels (dB). It is calculated as

$$SNR = 10\log_{10}\frac{\sum_{i,j} f^2_{(i,j)}}{\sum_{i,j} v^2_{(i,j)}} \quad (23)$$

where $v_{(i,j)}^{\ 2} = (d_{(i,j)} - f_{(i,j)})^2$, the nominator is the total square value of the original image and the denominator is the total square value of the noise.

The MSE is the measure of the total radiometric differences between two images [Hunt 1973; Eskicioglu and Fisher 1995] and defined as

$$MSE = \frac{1}{MN}\sum_{i=1}^{M}\sum_{j=1}^{N}(d_{ij} - f_{ij})^2 \quad (24)$$

5. SIMULATION RESULTS (BENZETİM SONUÇLARI)

The restoration results of the classical image restoration techniques are illustrated in Table 2 and in Figure 12. These processess contain three steps: the first step is the decomposition; the second step is the detail coefficient thresholding. For each level from 1 to N, a threshold was selected and hard thresholding was applied to the detail coefficients; the last step was the reconstruction.

Preprocessings in the classical techniques were employed in two ways. One is based on the WTW with the size of 3x3. The other is based on the entire image processing. When the entire image was applied to the classical techniques, the restoration performance was better than the WTW as seen in Table 2.

In general, the entire image was found better method in preprocessing. The WMF was found the most successful filter among the three techniques. It should be noticed that this process has two sequential steps in contrast to the FDF and the WT used only one step.

(a) restorated image with entire frame in FDF space

(b) restorated image with entire frame in WMF

(c) restorated image in WT

(d) restorated image with WTW in FFT space

(e) restorated image with WTW 3x3 image sized window in WMF

(f) restorated image with WTW in WT

Figure 12. Results for classical techniques. (Klasik teknilerin sonuçları)

Table 2. Similarity measures of classical image restoration techniques for different windowing processes. (Farklı pencereleme işlemleri için klasik resim iyileştirme tekniklerinin benzerlik ölçüm sonuçları).

Measures	Pre-processing	Defected Images	FDF	WMF	WT
SNR	WTP	13.229	14.51	17.97	14.60
	WTW	13.060	14.81	8.19	6.77
MSE	Entire image	64.600	46.40	20.90	45.40
	WTW	64.700	721.24	3317.7	4616.4
C	Entire image	0.9100	0.9460	0.9692	0.9513
	WTW	0.9102	0.9318	0.9497	0.8117

The results achieved from ANN models can be seen from Figures 13-17 and Tables 2-6. The results have shown that the image restorations with ANN models trained with the EDBD and the LMM have been found successful and efficient in this work. It needs to be emphasized that the approach presented in this work provides fascinating results without knowing the mathematical model of the random noise.

In the ANN models, increasing the size of the windowing decreases the similarities drastically as given in Table 3.

Table 3. The results of correlation measures for different sized WTWs. (Farklı WTW boyutlarında elde edilen korelasyon ölçüm sonuçları)

WTW sizes	ANN trained with	C
3x3	EDBD	0.9659
	LMM	0.9678
5x5	EDBD	0.9278
	LMM	0.4068

When the computational complexity in the classical and the ANN methods for restoration processes have been taken into account, the ANNs trained with the WTP data type provided the best results. In this case, the ANN models achieved the restoration twice better than the FDF and the WT according to C measure.

According to the learning algorithm selected, the suitable network configurations for 3x3 and 5x5 image sizes were 9x5x9 or 9x10x9 and 25x5x25 or 25x10x25, respectively. Table 3 shows the similarities between the original images and the images restorated with ANNs as given in Figure 13.

As can be seen from the results that ANN models trained with 3x3 image sized the unoverlapping WTW method was found more successful. Selecting large size windowing as 5x5 image caused undesired new edge information on the restorated image. For this reason, 3x3 image size windowing was used throughout in this work.

(a) 3x3 image sized and trained with EDBD

(b) 3x3 image sized and trained with LMM

(c) 5x5 image sized and trained with EDBD

(d) 5x5 image sized and trained with LMM

Figure 13. ANN results for different sized WTW windowing (farklı boyutlarda WTW pencereleme için YSA sonuçları)

The MSE results achieved from ANN models trained with LMM and EDBD for WTP and WTW were given in Table 4.

Table 4. MSE errors of different sets in training for both data types and learning algorithms. (Öğrenme sürecinde farklı öğrenme algoritması ve veri tiplerinde farklı kümlerin MSE hataları)

Training sets	MSE achieved from ANNs trained with (WTP)		MSE achieved from ANNs trained with (WTW)	
	EDBD	LMM	EDBD	LMM
Set#1	0.0038	0.0009	0.0328	0.0095
Set#2	0.0007	0.0008	0.0283	0.0169
Set#3	0.0068	0.0034	0.0099	0.0870
Set#4	0.0058	0.0032	0.0101	0.0093
Set#5	0.0057	0.0029	0.0071	0.1836
Set#6	0.0036	0.0016	0.0048	0.0071

Table 5. Similarity measure and number of epochs of test image with WTPs (WTP ile test edilmiş işlemler için epok sayısı ve benzerlik oranı)

Training sets	ANN trained with EDBD			ANN trained with LMM		
	NN no	Epoch	C	NN no	Epoch	C
Set#1	NN#1	918	0.8960	NN#7	18	0.8401
Set#2	NN#2	573	0.8725	NN#8	24	0.7697
Set#3	NN#3	435	0.9659	NN#9	100	0.9576
Set#4	NN#4	530	0.9642	NN#10	100	0.9678
Set#5	NN#5	199	0.9618	NN#11	100	0.9628
Set#6	NN#6	294	0.9604	NN#12	100	0.9606

The similarity measures between the original, as shown in Figure 10(a), and the restorated images were given in Table 5 with the correlations and the epochs of ANN models (NN#1-NN#12) trained with WTP data type. These test results of ANNs trained with the LMM and the EDBD were illustrated in Figures 14 and 15, respectively.

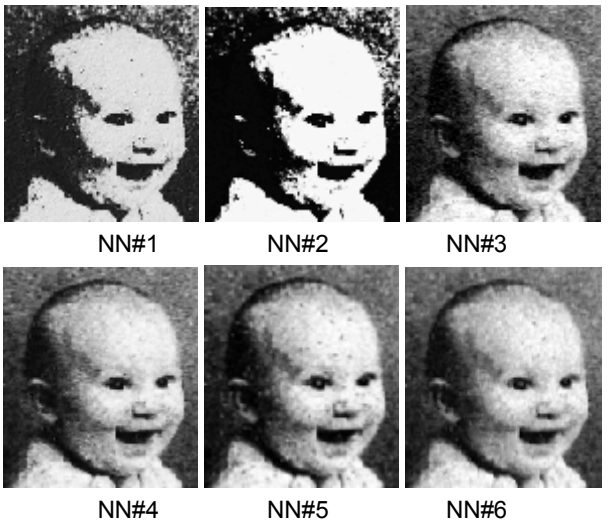

Figure 14. Restored images for each texture pair (WTP, ANNs trained with LMM). (Her bir resim çifti için iyileştirilmiş görüntüler)

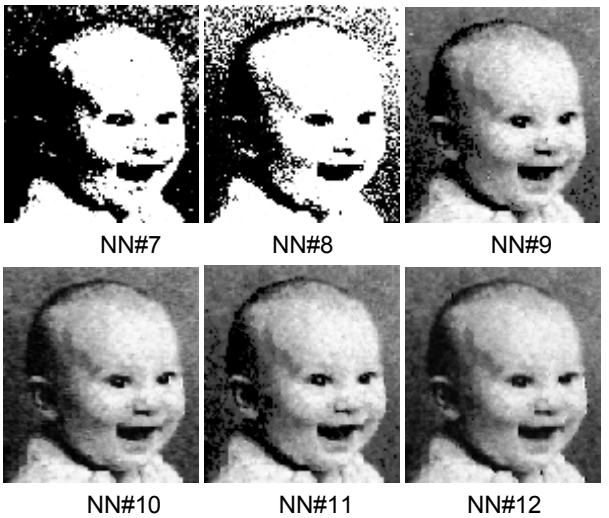

Figure 15. Restored images for each texture pair (WTP, ANNs trained with EDBD). (Her bir resim çifti için iyileştirilmiş görüntüler)

The similarity measures and the number of epochs belonging to the networks (NN#13-NN#24) were given in Table 6. The test results of neural models trained with the EDBD and the LMM were shown in Figures 16 and 17, respectively. As can be seen from Figure 16, the results obtained from the models NN#13 and NN#17 trained with the EDBD were acceptable.

Table 6. Similarity measure and number of epochs of test image with WTWs (WTW ile test edilmiş işlemler için epok sayısı ve benzerlik oranı)

Training sets	ANN trained with EDBD			ANN trained with LMM		
	NN no	Epoch	C	NN no	Epoch	C
Set#1	NN#13	1592	0.9116	NN#19	10	0.5210
Set#2	NN#14	1368	0.4484	NN#20	10	-0.037
Set#3	NN#15	339	0.7592	NN#21	10	0.2691
Set#4	NN#16	459	0.7515	NN#22	10	0.1897
Set#5	NN#17	389	0.9566	NN#23	10	0.1433
Set#6	NN#18	1089	0.9782	NN#24	10	0.1904

None of the neural models trained with the LMM algorithm was found successful in terms of the correlation measure (C).

As known well, C was a measure of the similarity and changed in the intervals (-1,+1). If C is more than 0.9107, it is said that the restoration is successful.

As a result, ANN models trained with the EDBD and the LMM algorithms using the texture pairs (Set#3-Set#6) were found successful for WTP in terms of the C measure.

When WTW data type is considered, the texture pairs (Set#1 and Set#5) were found successful the neural models trained with EDBD algorithm.

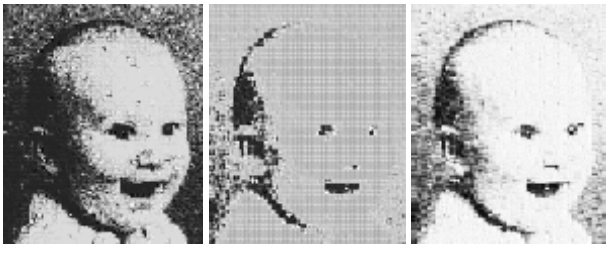

NN#13 NN#14 NN#15

NN#16 NN#17 NN#18

Figure 16. Restored images for each texture pair (WTW, ANNs trained with EDBD). (Her bir resim çifti için iyileştirilmiş görüntüler)

The images restored by the models NN#19, NN#20 and NN#24 in Figure 17 require the histogram equalization operation for the smooth illustrations.

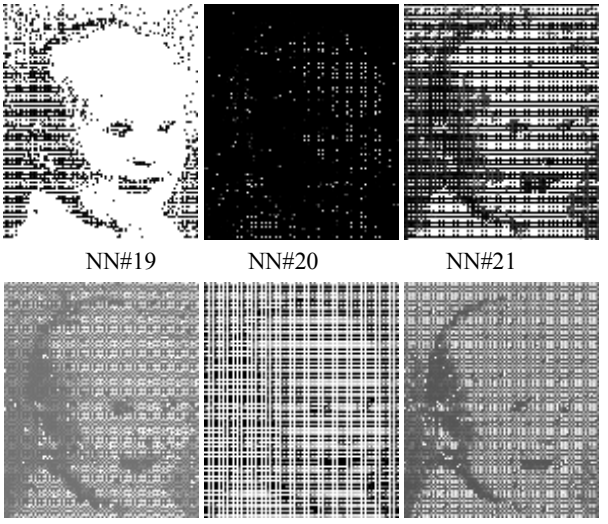

NN#19 NN#20 NN#21

NN#22 NN#23 NN#24

Figure 17. Restored images for each texture pair (WTW, ANNs trained with LMM). (Her bir resim çifti için iyileştirilmiş görüntüler)

6. CONCLUSIONS (SONUÇLAR)

A novel ANN based restoration approach has beeen successfully presented. This approach takes use of the learning capability of ANNs to learn the restoration of the images applied. This approach generates the noise-removed values from their noisy versions.

Simulation results have shown that the approach for gray-scale image restorations using ANNs presented in this work can effectively remove the noise and this significantly improves the visual quality of the degraded image. The proposed method requires no priori knowledge about the noise and needs only one level of signal decomposition to obtain very good restoration results. It should be emphasized that the approach presented in this work provides very good results without knowing the mathematical model of the noisy images. As in general, it is very clear from the restoration results that restoring images with ANNs provide simplicity, accuracy, less computational needs and ease of applicability.

This work can be concluded as:

- ANN models trained with the EDBD and the LMM have been found successful and efficient.
- ANN models provide very good results without knowing the mathematical model of the random noise.
- Among all techniques presented in this work, the ANN models have the simplest structure and the lowest computational complexity and also enable the close C measure to the WMF's one.
- When the computation time is considered, the WMF has the highest complexity because of its adaptability on each step.
- ANN models trained with the EDBD algorithm were found the most successful structures in terms of similarities for the both data types. Even the LMM had less training epoch, it required the large amount of memory and computation.
- When the both data types were considered, the WTP was found the most effective one to train the ANN models. Using the WTW data type did not provide acceptable results in the classical techniques and the ANNs. It also caused additional edge information occurring at the borders of the windows.
- The textures having systematically repeated primitives expressed the effect of random noise more realistically that is why the ANN models enabled more efficient solutions for the texture pairs presented in this work.
- The radiometric values of the textures matching the defected image values might increase the effectiveness. So this was very important to design an effective texture pairs for the effective restoration with the use of ANNs. If the radiometric values of the textures corresponded to the radiometric values of the defected image, the ANN models provided more effective solutions.
- In contrast to the classical techniques based on the mathematical properties of the noise, it was enough to estimate the defect of image visually for designing the textures of the input and output vectors. The success of ANN restoration depended on the designer's precise perception of the noise on the images.

This work also suggests that to get better performance in ANN training, WTP data type must be selected for precise restoration. Among six data sets, Set#3- Set#6 texture pairs were most appropriate for smooth restoration. It should be emphasized that using suitable similarity measure was also important for a well perception.

Disadvantages encountered in this approach were the selection of appropriate texture pairs, the observation of noise level, the preparation of input and output sets and the proper setting of the network configurations.

Finally, the approach suggested in this work might provide wide applications in Photogrammetry, Remote Sensing, Computer Vision, Telecommunication, etc. because of its simplicity and accuracy in restoration.

7. REFERENCES (KAYNAKLAR)

1) Ansari N, Zhang ZZ (1993) Generalised adaptive neural filters, IEE Electron. Lett. 29 (4), 342–343.
2) Azimisadjadi MR, Xiao RR, Yu X (1999) Neural-Network Decision Directed Edge-Adaptive Kalman Filter For Image Estimation, IEEE Transactions On Image Processing 8(4), 589-592.
3) Baltsavias EP (1994). Test and calibration procedures for image scanners, Archives of Photogrammetry and Remote Sensing (IAPRS) 30, 163-170.
4) Baltsavias EP, Bill R (1994) Scanners - a survey of current technologies and future needs, Archives of Photogrammetry and Remote Sensing (IAPRS) 30, 130-143.
5) Baltsavias EP, Kaeser C (1994) Evaluation and testing of the Zeiss SCAI roll film scanner, Archives of Photogrammetry and Remote Sensing (IAPRS) 32, 67-74.
6) Banham MR, Katsaggelos AK (1996) Spatially adaptive wavelet-based multiscale image restoration. IEEE Trans. Image Processing 5(4), 619-633.
7) Banham MR, Katsaggelos AK (1997) Digital image restoration. IEEE Signal Processing Magazine, 24-41.
8) Barto AG, Bradtke SJ, Singh SP (1995) Learning to Act using Real-Time Dynamic Programming, J. Artificial Intelligence, 72, 81-138.
9) Bedini L, Tonazzini A (1992) Image restoration preserving discontinuities: the Bayesian approach and neural networks, Image Vision Comput. 10 (2), 108–118.
10) Boykov Y, Veksler O, Zabih R (1998) A Variable Window Approach to Early Vision, IEEE Transactions On Pattern Analysis And Machine Intelligence 20(12), 1283-1294.
11) Bulsari AB, Saxen H (1982) A Feedforward Artificial Neural Network for System Identification of a Chemical Process, J. Syst. Eng. 1(1), 1-9.
12) Celebi ME, Guzelis C (1997) Image-Restoration Using Cellular Neural-Network, Electronics Letter 33(1), 43-45.
13) Chang SG, Bin Y, Vetterli M (2000a) Adaptive wavelet thresholding for image denoising and compression, IEEE Transactions on Image Processing 9(9), 1532-1546.
14) Chang SG, Bin Y, Vetterli M (2000b) Wavelet thresholding for multiple noisy image copies, IEEE Transactions on Image Processing, 9(9), 1631-1635.
15) Chellappa R, Kashyap RL (1982) Digital Image Restoration Using Spatial Interaction Models, IEEE

Trans. on Acoustics, Speech, and Signal Processing, 30(3), 461-471.

16) Chua W, Yang L (1988a) Cellular networks: applications, IEEE Trans. Circuits Systems 35 (10), 1273–1290.

17) Chua W, Yang L (1988b) Cellular networks: theory, IEEE Trans. Circuits Systems 35 (10), 1257–1272.

18) Demuth H, Beale M (1998) Neural Network Toolbox User's Guide, The Math Works, Inc., 1998.

19) Edelstein WA, Glover GH, Hardy CJ, Redington RW (1986) Intrinsic signal to noise ratio in NMR imaging, Magnetic Resonance in Medicine 3, 606-618.

20) Egmont-Petersen M, Ridder D, Handels H (2002) Image processing with neural networks-a review, Pattern Recognition 35, 2279–2301.

21) Elad M, Feuer A (1997) Restoration of a single superresolution image form several blurred, noisy and undersampled measured images. IEEE Transactions on Image Processing 6(12), 1646-1658;

22) Eskicioglu AM, Fisher PS (1995) Image Quality Measures and Their Performance, IEEE Transactions on Communications, 43(12), 2959-2965.

23) Figueiredo MAT, Leitao JMN (1994) Sequential and parallel image restoration: neural network implementations, IEEE Trans. Image Process. 3(6), 789–801.

24) Fletcher R (1980) Unconstrained Optimization, Practical Methods of Optimisation, 1, Wiley.

25) Flusser J, Suk T (1998) Degraded Image Analysis: An Invariant Approach, IEEE Transactions on Pattern Analysis and Machine Intelligence 20(6), 590-603.

26) Galatsanos NP, Chin RT (1991). Digital Restoration of Multichannel Images, IEEE Trans. Signal Processing 39(10), 2237-2252.

27) Gill PG, Murray W, Wright VH (1981) Practical Optimisation, Academic Press.

28) Greenhil D, Davies ER (1994) Relative electiveness of neural networks for image noise suppression, Proceedings of the Pattern Recognition in Practice IV, Vlieland, 367–378.

29) Guan L (1996) An Optimal Neuron Evolution Algorithm For Constrained Quadratic-Programming In Image-Restoration, IEEE Transactions On Systems Man And Cybernetics Part A-Systems And Humans 26(4), 513-518.

30) Guan L, Anderson JA, Sutton JP (1997) A network of networks processing model for image regularization, IEEE Trans. Neural Networks, 8 (1), 169–174.

31) H. C. Andrews, B. R. Hunt (1977) Digital Image restoration. Englewood Cliffs, NJ: Prentice-Hall.

32) Hanek H, Ansari N (1996) Speeding up the generalized adaptive neural filters, IEEE Trans. Image Process. 5(5), 705–712.

33) Haykın S (1994) Neural Networks: A Comprehensive Foundation. Macmillan College Publishing Company, ISBN 0-02-352761-7, New York, USA.

34) Huang X, Woolsey GA (2000) Image denoising using Wiener filtering and wavelet thresholding, IEEE International Conference on Multimedia and Expo 3, 1759-1762.

35) Hunt B (1973) The application of constrained least squares estimation to image restoration by digital computer, IEEE Trans. on Communications, C-22, 805-812.

36) Keller PE, Kouzes RT, Kangas LJ (1993) Applications of neural networks to Real-Time Data Processing at the Environmental and Molecular Sciences Laboratory, ***Conference Record of the Eigth Conference on Real-Time Computer Applications in Nuclear, Particle and Plasma Physics***, 438-440.

37) Krell G, Herzog A, Michaelis B (1996) Real-Time Image Restoration with an Artificial Neural Network, Proc. of the International Conference on Neural Networks ICNN '96, Washington, 1552-1557.

38) Kundur D (1995) Blind Deconvolution of Still Images using Recursive Inverse Filtering, MSc. Thesis, Dept. of Electrical & Computer Engineering, University of Toronto.

39) Kundur D, Hatzinakos D (1996) Blind Image Restoration via Recursive Filtering using Deterministic Constraints, Proc. IEEE Int. Conf. On Acoustics, Speech and Signal Processing, 1996; 4, 2283-2286, Atlanta, USA.

40) Lagendijk RL, Biemond J, Boekee DE (1988) Regularized iterative image restoration with ringing reduction, IEEE Trans. Acoust., Speech, Signal Processing 36, 1874-1887.

41) Lee CC, Degyvez JP (1996) Color image processing in a cellular neural-network environment, IEEE Trans. Neural Networks, 7 (5), 1086–1098.

42) Lee JB Woodyatt AS and Berman M (1990) Enhancement of high spectral resolution remote sensing data by a noise-adjusted principal components transform, IEEE Trans. Geosci. Remote Sensing, 28, 295-304.

43) Li SZ (1998) MAP Image Restoration and Segmentation by Constrained Optimization, IEEE Transactions On Image Processing 7(12), 1730-1735.

44) Liguni Y et. Al (1992) A real-time learning algorithm for a multilayered neural network based on the extended Kalman filter, IEEE Trans. Signal. Proc. 40(4), 959-966.

45) Mansour AKB, Kawamoto M, Ohnish N (1998) A fast algorithm for blind separation of sources based on the cross-cumulant and Levenberg-Marquardt method In Fourth International Conference on Signal Processing (ICSP'98), Beijing, China, 323-326.

46) Marquardt DW (1963) An Algorithm For Least-Squares Estimation Of Nonlinear Parameters. J. Soc. Ind. Appl. Math., 11, 431-441.

47) Moulin P (1995) A Multiscale relaxation Algorithm for SNR Maximization in Nonorthogonal Subband Coding, IEEE Transactions on Image Processing, 4(9), 1269-1281.

48) Murtagh F, Starck JL (19952) Bijaoui A. Image restoration with noise suppression using a multiresolution support, Astronomy and Astrophysics, Supplement Series 112, 179-189.

49) NeuralWare Handbook (1996) Neural Computing, A technology Handbook for Professional II/PLUS and NeuralWorks Explorer, Pittsburgh. USA.

50) Nossek JA, Roska T (1993) Special issue on Cellular Neural Networks, IEEE Trans. Circuits Systems, I. Fundamental Theory and Applications, 40 (3)

51) Paik JK, Katsaggelos AK (1992) Image restoration using a modified Hopfield network, IEEE Trans. Image Process. 1 (1), 49–63.

52) Paik JK, Katsaggelos AK (1992). Image restoration using a modified Hopfield network, IEEE Trans. Image Processing 1(1), 49-63.

53) Perez-Minana E, Wallace D, Fisher RB (1993) Stochastic Image Restoration: Clean Images and Their Likelihood, Proceedings 6th International Conference on Industrial and Engineering Applications of Artificial Intelligence and Expert Systems, 518-521.

54) Pham DT, Sagiroglu S (1996) Three Methods of Training Multi-Layer Perceptrons to Model a Robot Sensor, Robotica, 13, 531-538.

55) Phoha VV, Oldham WJB (1996) Image recovery and segmentation using competitive learning in a layered network, IEEE Trans. on Neural Networks 7(4), 843–856.

56) Qian W, Kallergi M, Clarke LP (1993) Order statistic-neural network hybrid filters for gamma-camera-bremsstrahlung image restoration, IEEE Trans. Med. Imaging 12(1), 58–64.

57) R. C. Gonzalez, R. E. Woods (1992) Digital Image Processing, Addison-Wesley.

58) Ridder D, Duin RPW, Verbeek, PW, et al. (1999) The applicability of neural networks to non-linear image processing, Pattern Anal. Appl. 2(2), 111–128.

59) Ripley BD (1996) Pattern Recognition and Neural Networks, Cambridge University Press. ISBN 0-521 46086-7.

60) Schomberg H, Timmer J (1982) The Gridding Method for Image Reconstruction by Fourier Transformation, IEEE Transactions on Medical Imaging 14, 596-607.

61) Simpson PK (1990) Artificial Neural Systems Foundation, Paradigms, Application and Implementation, Permagnon Press, ISBN-08-037895-1.

62) Skrzypek K, Karpluz W (1992) Neural Network in Vision and Pattern Recognition, Singapore, River Edge, NJ.

63) Sonka M, Hlavac V, Boyle R (19992) Image processing, analysis, and machine vision, Second Edition, Brook/Cole Publishing Company, Pasific Grove, USA.

64) Steriti RJ, Fiddy MA (1993) Regularised image reconsruction using SVD and a neural network method for matrix inversion, IEEE Trans. Signal. Proc. 41(10), 3074-3077.

65) Strak H. Image Recovery Theory and Application, Academic Press Inc., Florida, 1987; 1-26, 128-155.

66) Sun X, Wu F, Li S, Gao W, Zhang YQ (2001) Macroblock-based temporal-SNR progressive fine granularity scalable video coding, IEEE International Conference on Image Processing (ICIP), Thessaloniki, Greece.

67) Sun YL, Yu S (1995) Improvement on performance of modi1ed Hopfield neural network for image restoration, IEEE Trans. Image Process., 4(5), 683–692.

68) Tekalp AM, Pavlovic G (1990). Multichannel Image Modeling and Kalman Filtering for Multispectral Image Restoration, IEEE Trans. Signal Processing 19(3), 221-232.

69) Vrhel MJ, Unser M (1999) Multichannel Restoration with Limited A Priori Information, IEEE Transactions on Image Processing 8(4), 527-536.

70) Wang RK, Chatwin CR, Young RCD (1995) Assessment of a Wiener Filter Synthetic Discriminant Function for Optical Correlation, Optics And Lasers In Engineering 22(1), 33-51.

71) Weng J (1993). Image matching using the windowed Fourier phase. International Journal of Computer Vision 11(2), 211-236.

72) Wilson R, Calway AD, Pearson ERS (1992) A Generalized Wavelet Transform for Fourier Analysis: the Multiresolution Fourier Transform and its Application to Image and Audio Signal Analysis, IEEE Transactions on Information Theory 38(2), 674-690.

73) Wong HS, Guan L (1997) Adaptive Regularization In Image-Restoration Using A Model- Based Neural-Network, Optical Engineering 36(12), 3297-3308.

74) Woo W, Kim J, Jeong H, Hong K (1991) Stochastic Model for Range Image restoration and Segmentation, Journal of the KITE 28-B(6), 49-59.

75) Zamparelli M (1997) Genetically trained cellular neural networks, Neural Networks, 10(6), 1143–1151.

76) Zhang H, Nosratinia A, Wells RO (2000) Image denoising via wavelet-domain spatially adaptive FIR Wiener filtering, IEEE International Conference on Acoustics, Speech, and Signal Processing, Proceedings of ICASSP 4, 2179-2182,

77) Zhang ZZ, Ansari N (1996) Structure and properties of generalized adaptive neural filters for signal enhancement, IEEE Trans. Neural Networks 7(4), 857–868.

78) Zhao JY, Yu DH (1999) A New Approach For Medical Image-Restoration Based On CNN, International Journal Of Circuit Theory And Applications 27(3), 339-346.

79) Zhou YT, Chellapa A, Vaid A, Jenkins BK (1988) Image Restoration Using a Neural Network. IEEE Transactions on Acoustics, Speech, and Signal Processing 36(7), 1141-1151